Dalton Transactions

COMMUNICATION

View Article Online
View Journal | View Issue

Cite this: *Dalton Trans.*, 2019, **48**, 854

Received 16th November 2018,
Accepted 12th December 2018

DOI: 10.1039/c8dt04557g

rsc.li/dalton

Microwave-assisted synthesis: from a mononuclear {Co^{II}} complex to {Co^{II}_9} solvomorphs†

Alexandra Collet, Claire Wilson and Mark Murrie *

We report a new {Co^{II}_9} complex with an unprecedented structure and its solvated analogue, using microwave heating to tune the synthesis and improve the product selectivity.

Polymetallic 3d and/or 4f complexes have attracted a great deal of interest due to their interesting properties and applications in scientific fields such as molecule-based magnets, magnetic refrigerants, water oxidation electrocatalysts and MRI contrast agents.[1] Therefore, the need to synthesise and characterise these complexes continues to grow. Microwave-assisted synthesis is being employed more frequently in inorganic synthesis, instead of conventional heating in an oven, due to three main advantages: reduced reaction times, increased yields and product selectivity.[2] However, there are still only limited examples of polynuclear coordination complexes synthesised using this method.[3,4]

We have investigated the coordination chemistry of the polydentate ligand bicine (H_3bic, *N*,*N*-bis(2-hydroxyethyl) glycine)[5] with Co^{II}. Herein, we report a new, microwave-assisted synthetic procedure for the previously reported [Co^{II}(H_2bic)Cl] (**1**)[6] (Fig. 1 left). Furthermore, we present a new nonanuclear complex [Co^{II}_9(Hbic)$_4$(bic)$_2$Cl$_4$] (**2**), with an unprecedented metallic core (Fig. 1 right), and its solvated analogue [Co^{II}_9(Hbic)$_4$(bic)$_2$Cl$_4$]·12H_2O (**2**·12H_2O), by adjusting the synthetic procedure used for **1**. The reaction of $CoCl_2$·6H_2O with bicine and NEt_3 in EtOH under solvothermal conditions, resulted in a mixture of the complexes **1** (pink block-like crystals), **2** (blue block-like crystals) and **2**·12H_2O (blue needle-like crystals). However, by using microwave-assisted heating the selectivity is improved (see Scheme 1) and **1**, **2** and **2**·12H_2O can be isolated separately. The full experimental procedure is included in the ESI.†

Complex **1** crystallises in the orthorhombic *Pbca* space group,[6] while single-crystal X-ray diffraction for **2** and **2**·12H_2O revealed that the complexes crystallise in the monoclinic $P2_1/n$

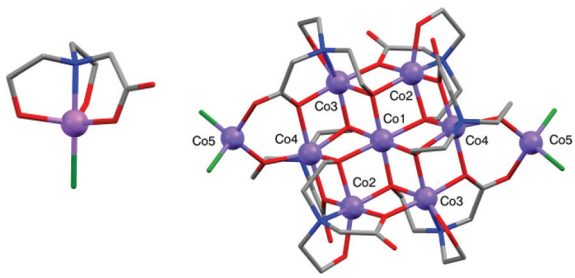

Fig. 1 The molecular structure of **1** (left) and [Co^{II}_9(Hbic)$_4$(bic)$_2$Cl$_4$] (right). Colour code: Co^{II}: violet, Cl: green, O: red, N: blue, C: grey. Hydrogen atoms are omitted for clarity.

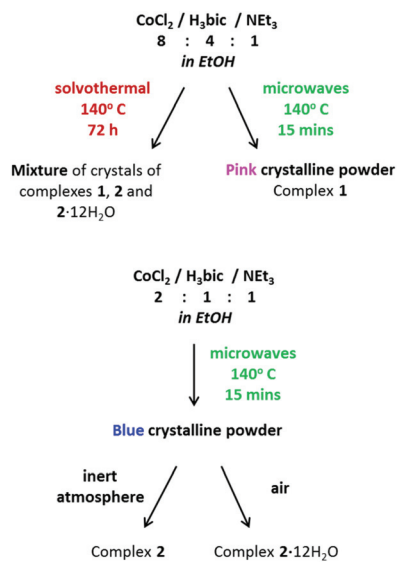

Scheme 1 The synthetic procedure followed to isolate complexes **1**, **2** and **2**·12H_2O.

WestCHEM, School of Chemistry, University of Glasgow, University Avenue, Glasgow G12 8QQ, UK. E-mail: mark.murrie@glasgow.ac.uk

†Electronic supplementary information (ESI) available. CCDC 1878568–1878569. For ESI and crystallographic data in CIF or other electronic format see DOI: 10.1039/c8dt04557g

and trigonal $R\bar{3}$ space groups, respectively. The crystallographic data for **2** and **2**·12H_2O can be found in Table S1 (see ESI†). The Co^{II} centre in complex **1** is five-coordinate and adopts a distorted trigonal bipyramidal (TBP) geometry, with one singly deprotonated bicine ligand and one terminal Cl^- ligand. Continuous shape measures (CShMs),[7] which provide an estimate of the distortion from the ideal TBP geometry for the Co^{II}, give a value of 1.42 (where 0 corresponds to the ideal polyhedron), confirming a significant distortion (Table S2 and Fig. S1, ESI†). Bond Valence Sum (BVS) analysis was used to confirm the oxidation state of Co^{II}.[8] Intermolecular hydrogen bonds occur between the hydroxyl groups and the carboxylate groups of neighbouring molecules, forming a two-dimensional network (Fig. S2, ESI†). The shortest intermolecular Co···Co′ distances are ~4.8 Å.[6]

The new nonanuclear complex **2** adopts an unprecedented structural motif which consists of a $\{Co_7^{II}\}$ disk-like core with two additional tetrahedral Co^{II} centres. There are only a few examples of $\{Co_9^{II}\}$ complexes and none of them adopt a similar topology as the complex presented here.[9,10] The crystal packing of **2** and **2**·12H_2O is different (Fig. 2) due to the co-crystallised molecules of water. Small differences are observed in the distortion of the geometries of the cobalt centres and CShMs values for all Co^{II} centres for **2** and **2**·12H_2O were calculated with the programme SHAPE[11] (Tables S3 and S4, ESI†). Seven Co^{II} centres adopt distorted octahedral geometries, while the remaining two adopt slightly distorted tetrahedral geometries. All nine cobalt centres in **2** are in the +2 oxidation state, as confirmed by BVS analysis.[8] Five Co^{II} (Co1, Co2, Co2′, Co3, Co3′) centres define a plane while Co4, Co4′, Co5 and Co5′ are located outside this plane (Fig. S3†). This puckered $\{Co_7^{II}\}$ motif is also found in $\{Co_7^{II}\}$ with similar donor atoms and is not likely to be a result of the extra Co5/Co5′ centres.[12] Intramolecular interactions are present between the hydroxyl and carboxylate groups of **2** and **2**·12H_2O. In the solvomorph **2**·12H_2O intermolecular interactions occur between the hydroxyl and carboxylate groups of neighbouring molecules with the molecules of solvent (see Fig. S4†).

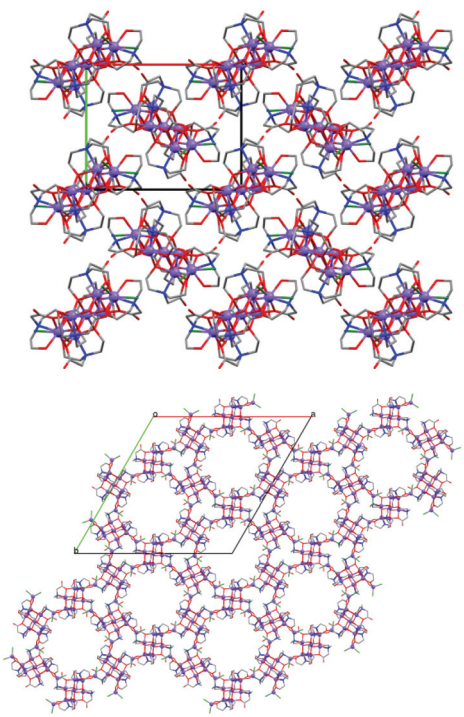

Fig. 2 The crystal packing of **2** (top) and **2**·12H_2O (bottom) along the crystallographic *c*-axis. The water molecules inside the channels of **2**·12H_2O are omitted for clarity. Colour code: Co^{II}: violet, Cl: green, O: red, N: blue, C: grey. Hydrogen atoms are omitted for clarity.

In order to examine if it is possible to isolate the three compounds separately we investigated further by making various changes to the synthetic procedure (*e.g.* the amount of base, the cobalt salt, the reaction time and/or temperature used in the solvothermal reactions). However, solvothermal conditions always led to a mixture of crystals or crystalline precipitates; therefore, we investigated microwave heating instead. Under microwave heating, in EtOH with a ligand to base ratio ~4 : 1 a pink crystalline powder is isolated, whereas when the ligand to base ratio is changed to 1 : 1, a blue crystalline powder is formed (for full experimental description see ESI†). Both products were collected by filtration and dried in air, and powder X-ray diffraction (Fig. 3) revealed that the pink and blue products corresponded to complexes **1** and **2**·12H_2O, respectively. Moreover, when the blue crystalline product is instead collected by filtration and dried under a nitrogen atmosphere, complex **2** is obtained, as confirmed by powder X-ray diffraction (Fig. 3). Hence, the $\{Co_9^{II}\}$ crystal packing (Fig. 2) depends on the drying process (Scheme 1) *i.e.* drying under an inert atmosphere (glove bag) gives **2**, whereas drying in air gives **2**·12H_2O. Therefore, depending on which drying process is applied, we are able to control which $\{Co_9^{II}\}$ solvomorph is formed.

Variable temperature dc susceptibility data were collected for **1**, **2** and **2**·12H_2O in a field of 1000 Oe in the 290–2 K temperature range (Fig. 4 and 5). At 290 K the $\chi_M T$ value of **1** is 2.57 $cm^3\ mol^{-1}$ K, higher than the expected $\chi_M T$ = 1.88 $cm^3\ mol^{-1}$ K for a high-spin Co^{II} (S = 3/2 and g = 2), indicating a spin–orbit coupling contribution. Upon cooling, $\chi_M T$ decreases slowly until ~12 K, then increases slightly at 8 K (2.27 $cm^3\ mol^{-1}$ K) and drops again to a minimum at 2 K. This behaviour indicates the presence of magnetic anisotropy and weak ferromagnetic intermolecular interactions[13] (hydrogen bonds are present and the Co^{II} centres of neighbouring molecules in **1** are close ~4.8 Å), although we were unable to obtain a satisfactory ferromagnetic zJ term when included in the fit. Magnetisation *versus* field plots at 2, 4 and 6 K did not saturate, a further indication of the presence of magnetic anisotropy (Fig. 4 inset). The dc magnetic susceptibility data and the magnetisation curves of **1** were fitted simultaneously using the programme PHI[14] (Fig. 4). Attempts to fit the data with an anisotropic g value were not successful, while using a positive D did not produce reasonable results, which is a strong indication that an easy-axis magnetic anisotropy is present here. This assumption is reasonable, since the use of a tripodal

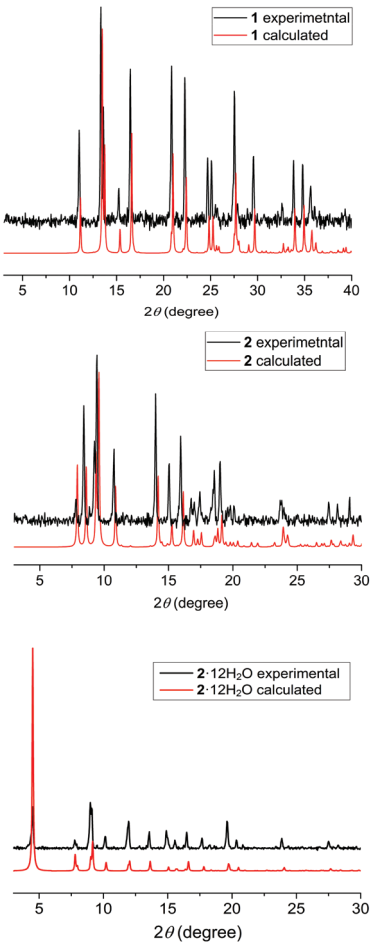

Fig. 3 The powder X-ray diffraction patterns of **1** (3–40°), **2** (3–30°) and **2**·12H_2O (3–30°). The red lines represent the calculated powder X-ray diffraction pattern for each complex and the black lines the experimental ones. All the experimental PXRD patterns were measured at ambient temperature, while the calculated patterns are generated from the single-crystal data collected at 296 K for **1**,[6] and 100 K for **2** and **2**·12H_2O.

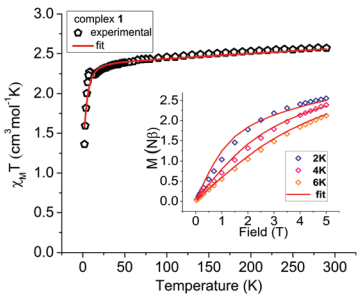

Fig. 4 Variable temperature dc susceptibility data for **1** in a field of 1000 Oe from 290–2 K. Inset: Magnetisation *versus* field plot at temperatures 2, 4 and 6 K for **1**. The red solid lines represent the fit (see text for details).

ligand can enforce C_3 symmetry and, as has been seen in previously reported examples, an easy-axis anisotropy ($D < 0$) can be promoted.[15] The extracted parameters from the fitting of

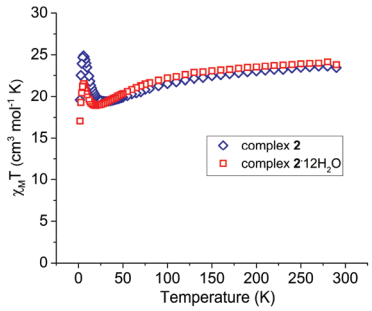

Fig. 5 Variable temperature dc susceptibility data for **2** (blue) and **2**·12H_2O (red) in a field of 1000 Oe from 290–2 K.

the data are: g = 2.25, D = −5.92 (±0.24) cm^{-1} and E = −1.32 (±0.09) cm^{-1}, with χ_{TIP} = 0.0006 cm^3 mol^{-1} for a Co^{II} in TBP geometry.[16]

The $\chi_M T$ values at room temperature for **2** and **2**·12H_2O are 23.4 and 23.8 cm^3 mol^{-1} K, respectively, which are higher than the theoretical spin-only value $\chi_M T$ = 16.9 cm^3 mol^{-1} K for nine non-interacting high-spin Co^{II} (S = 3/2 and g = 2), indicating a spin–orbit coupling contribution. $\chi_M T$ slowly decreases with the decrease of temperature until 26 and 19 K for **2** and **2**·12H_2O, due to the presence of spin–orbit coupling; then $\chi_M T$ increases sharply at 6 K for both complexes reaching the values of 26.2 and 21.5 cm^3 mol^{-1} K for **2** and **2**·12H_2O respectively, which can be attributed to the presence of ferromagnetic exchange interactions. Finally $\chi_M T$ decreases for both complexes at low temperature, due to zero-field splitting (ZFS) and/or intermolecular antiferromagnetic interactions.

Magnetisation *versus* field plots at 2, 4 and 6 K did not saturate for both complexes, an indication of the presence of magnetic anisotropy (Fig. S5†). This behaviour is in agreement with other polynuclear Co^{II}-based complexes.[4,10,17] It was not possible to fit the data due to the complexity of the system and the presence of octahedral Co(II).

Ac susceptibility measurements were performed for all complexes in order to examine if there is slow relaxation of the magnetisation. Complex **1** does not display any out-of-phase ac signal in zero or an applied dc field. This could be attributed to the significant distortion of the TBP geometry around Co^{II}, the presence of hydrogen bonds between neighbouring molecules and/or the short intermolecular Co···Co′ distances (~4.8 Å). Complex **2** displays only the onset of out-of-phase signals in zero or an applied 2000 Oe dc field (Fig. S6†), while complex **2**·12H_2O does not display any out-of-phase signals in zero or an applied dc field (Fig. S7, ESI†). The different behaviour between the two $\{Co_9^{II}\}$ complexes could be ascribed to the subtle structural differences between the two complexes (slightly different distortion of the Co^{II} centres, Tables S3 and S4, ESI†) and/or the absence of solvent molecules in the crystal lattice of **2**. It has been previously reported that the absence or change of solvent can drastically affect the magnetic properties of a complex.[18]

In conclusion, we report a new $\{Co_9^{II}\}$ complex $[Co_9^{II}(Hbic)_4(bic)_2Cl_4]$ (**2**), which extends the well-known $\{Co_7^{II}\}$

disk-like structure[12,19] with two adjacent tetrahedral Co^{II} centres, and its solvomorph $[Co^{II}_9(Hbic)_4(bic)_2Cl_4]\cdot 12H_2O$ (**2**·$12H_2O$), and a new synthesis for $[Co^{II}(H_2bic)Cl]$ (**1**).[6] In particular, this work highlights the potential of microwave-assisted synthesis in the synthesis of polymetallic complexes using polydentate ligands where bench or solvothermal synthesis leads to a mixture of products. We believe that this approach will prove applicable to a wide range of systems.

Conflicts of interest

There are no conflicts to declare.

Acknowledgements

We thank the University of Glasgow for funding and the EPSRC UK National Crystallography Service at the University of Southampton for the collection of the crystallographic data.[20]

Notes and references

1 J. Ferrando-Soria, J. Vallejo, M. Castellano, J. Martínez-Lillo, E. Pardo, J. Cano, I. Castro, F. Lloret, R. Ruiz-García and M. Julve, *Coord. Chem. Rev.*, 2017, **339**, 17–103; Y.-Z. Zheng, G.-J. Zhou, Z. Zheng and R. E. P. Winpenny, *Chem. Soc. Rev.*, 2014, **43**, 1462–1475; R. Brimblecombe, G. F. Swiegers, G. C. Dismukes and L. Spiccia, *Angew. Chem., Int. Ed.*, 2008, **47**, 7335–7338; G. Maayan, N. Gluz and G. Christou, *Nat. Catal.*, 2018, **1**, 48–54; G. Guthausen, J. R. Machado, B. Luy, A. Baniodeh, A. K. Powell, S. Krämer, F. Ranzinger, M. P. Herrling, S. Lackner and H. Horn, *Dalton Trans.*, 2015, **44**, 5032–5040; M. Murrie, *Polyhedron*, 2018, **150**, 1–9.

2 J. Zhao and W. Yan, in *Modern Inorganic Synthetic Chemistry*, ed. R. Xu, W. Pang and Q. Huo, Elsevier, Amsterdam, 2011, pp. 173–195.

3 C. J. Milios, A. Prescimone, J. Sanchez-Benitez, S. Parsons, M. Murrie and E. K. Brechin, *Inorg. Chem.*, 2006, **45**, 7053–7055; C. J. Milios, A. Vinslava, A. G. Whittaker, S. Parsons, W. Wernsdorfer, G. Christou, S. P. Perlepes and E. K. Brechin, *Inorg. Chem.*, 2006, **45**, 5272–5274; M.-H. Zeng, Y.-L. Zhou, W.-X. Zhang, M. Du and H.-L. Sun, *Cryst. Growth Des.*, 2010, **10**, 20–24; Y.-L. Zhou, M.-H. Zeng, L.-Q. Wei, B.-W. Li and M. Kurmoo, *Chem. Mater.*, 2010, **22**, 4295–4303; L.-Q. Wei, K. Zhang, Y.-C. Feng, Y.-H. Wang, M.-H. Zeng and M. Kurmoo, *Inorg. Chem.*, 2011, **50**, 7274–7283; K. Zhang, J. Dai, Y.-H. Wang, M.-H. Zeng and M. Kurmoo, *Dalton Trans.*, 2013, **42**, 5439–5446; H.-G. Jin, X. Jiang, I. A. Kühne, S. Clair, V. Monnier, C. Chendo, G. Novitchi, A. K. Powell, K. M. Kadish and T. S. Balaban, *Inorg. Chem.*, 2017, **56**, 4864–4873.

4 L.-Q. Wei, B.-W. Li, S. Hu and M.-H. Zeng, *CrystEngComm*, 2011, **13**, 510–516.

5 K. Graham, A. Darwish, A. Ferguson, S. Parsons and M. Murrie, *Polyhedron*, 2009, **28**, 1830–1833.

6 Y. Zhou, X. Liu, Q. Wang, L. Wang and B. Song, *Acta Crystallogr., Sect. E: Crystallogr. Commun.*, 2016, **72**, 1463–1467.

7 M. Pinsky and D. Avnir, *Inorg. Chem.*, 1998, **37**, 5575–5582; S. Alvarez and M. Llunell, *J. Chem. Soc., Dalton Trans.*, 2000, 3288–3303.

8 N. E. Brese and M. O'Keeffe, *Acta Crystallogr., Sect. B: Struct. Sci.*, 1991, **47**, 192–197.

9 A. Tsohos, S. Dionyssopoulou, C. P. Raptopoulou, A. Terzis, E. G. Bakalbassis and S. P. Perlepes, *Angew. Chem., Int. Ed.*, 1999, **38**, 983–985; L. N. Dawe, K. V. Shuvaev and L. K. Thompson, *Inorg. Chem.*, 2009, **48**, 3323–3341; E. Fursova, O. Kuznetsova, V. Ovcharenko, G. Romanenko, V. Ikorskii, I. Eremenko and A. Sidorov, *Polyhedron*, 2007, **26**, 2079–2088; S. K. Langley, M. Helliwell, S. J. Teat and R. E. P. Winpenny, *Dalton Trans.*, 2012, **41**, 12807–12817; W. Shentang, B. Yanfeng, H. Xinxin, Z. Xiaofei and L. Wuping, *Z. Anorg. Allg. Chem.*, 2017, **643**, 160–165.

10 G. S. Papaefstathiou, A. K. Boudalis, T. C. Stamatatos, C. J. Milios, C. G. Efthymiou, C. P. Raptopoulou, A. Terzis, V. Psycharis, Y. Sanakis, R. Vicente, A. Escuer, J.-P. Tuchagues and S. P. Perlepes, *Polyhedron*, 2007, **26**, 2089–2094.

11 S. Alvarez, D. Avnir, M. Llunell and M. Pinsky, *New J. Chem.*, 2002, **26**, 996–1009; C. Jordi, A. Pere and A. Santiago, *Chem. – Eur. J.*, 2004, **10**, 190–207.

12 R. Pattacini, P. Teo, J. Zhang, Y. Lan, A. K. Powell, J. Nehrkorn, O. Waldmann, T. S. A. Hor and P. Braunstein, *Dalton Trans.*, 2011, **40**, 10526–10534; S.-H. Zhang, L.-F. Ma, H.-H. Zou, Y. G. Wang, H. Liang and M. H. Zeng, *Dalton Trans.*, 2011, **40**, 11402–11409; R. Modak, Y. Sikdar, A. E. Thuijs, G. Christou and S. Goswami, *Inorg. Chem.*, 2016, **55**, 10192–10202.

13 Y.-Z. Zhang, W. Wernsdorfer, F. Pan, Z.-M. Wang and S. Gao, *Chem. Commun.*, 2006, 3302–3304; T. Jurca, A. Farghal, P.-H. Lin, I. Korobkov, M. Murugesu and D. S. Richeson, *J. Am. Chem. Soc.*, 2011, **133**, 15814–15817; F. Habib, O. R. Luca, V. Vieru, M. Shiddiq, I. Korobkov, S. I. Gorelsky, M. K. Takase, L. F. Chibotaru, S. Hill, R. H. Crabtree and M. Murugesu, *Angew. Chem., Int. Ed.*, 2013, **52**, 11290–11293.

14 N. F. Chilton, R. P. Anderson, L. D. Turner, A. Soncini and K. S. Murray, *J. Comput. Chem.*, 2013, **34**, 1164–1175.

15 I. Nemec, R. Marx, R. Herchel, P. Neugebauer, J. van Slageren and Z. Trávníček, *Dalton Trans.*, 2015, **44**, 15014–15021; R. Ruamps, L. J. Batchelor, R. Guillot, G. Zakhia, A.-L. Barra, W. Wernsdorfer, N. Guihéry and T. Mallah, *Chem. Sci.*, 2014, **5**, 3418–3424; D. Schweinfurth, J. Krzystek, M. Atanasov, J. Klein, S. Hohloch, J. Telser, S. Demeshko, F. Meyer, F. Neese and B. Sarkar, *Inorg. Chem.*, 2017, **56**, 5253–5265; T. J. Woods, M. F. Ballesteros-Rivas, S. Gómez-Coca, E. Ruiz and K. R. Dunbar, *J. Am. Chem. Soc.*, 2016, **138**, 16407–16416; S. Tripathi, A. Dey, M. Shanmugam, R. S. Narayanan and V. Chandrsekhar, in

Topics in Organometallic Chemistry, Springer, Berlin, Heidelberg, 2018, pp. 1–41.

16 R. Herchel and R. Boča, *Dalton Trans.*, 2005, 1352–1353; J. S. Wood, *J. Chem. Soc. A*, 1969, 1582–1586.

17 X.-T. Wang, B.-W. Wang, Z.-M. Wang, W. Zhang and S. Gao, *Inorg. Chim. Acta*, 2008, **361**, 3895–3902; S.-H. Zhang, R.-X. Zhao, G. Li, H.-Y. Zhang, C.-L. Zhang and G. Muller, *RSC Adv.*, 2014, **4**, 54837–54846; T. Singha Mahapatra, D. Basak, S. Chand, J. Lengyel, M. Shatruk, V. Bertolasi and D. Ray, *Dalton Trans.*, 2016, **45**, 13576–13589.

18 J.-Y. Ge, L. Cui, J. Li, F. Yu, Y. Song, Y.-Q. Zhang, J.-L. Zuo and M. Kurmoo, *Inorg. Chem.*, 2017, **56**, 336–343; C.-M. Liu, D.-Q. Zhang and D.-B. Zhu, *Sci. Rep.*, 2017, **7**, 15483; W.-Y. Zhang, Y.-Q. Zhang, S.-D. Jiang, W.-B. Sun, H.-F. Li, B.-W. Wang, P. Chen, P.-F. Yan and S. Gao, *Inorg. Chem. Front.*, 2018, **5**, 1575–1586.

19 A. B. Canaj, L. E. Nodaraki, K. Ślepokura, M. Siczek, D. I. Tzimopoulos, T. Lis and C. J. Milios, *RSC Adv.*, 2014, **4**, 23068–23077.

20 S. J. Coles and P. A. Gale, *Chem. Sci.*, 2012, **3**, 683–689.